Earth and Planetary Science Letters 458 (2017) 349–356

Contents lists available at ScienceDirect

Earth and Planetary Science Letters

www.elsevier.com/locate/epsl

Impact of uncertain reference-frame motions in plate kinematic reconstructions: A theoretical appraisal

Giampiero Iaffaldano [a,*], Seth Stein [b]

[a] Department of Geosciences and Natural Resource Management, University of Copenhagen, Denmark
[b] Department of Earth and Planetary Sciences, Northwestern University, USA

ARTICLE INFO

Article history:
Received 7 April 2016
Received in revised form 28 October 2016
Accepted 1 November 2016
Available online 17 November 2016
Editor: P. Shearer

Keywords:
finite rotations
reference frames
plate motions

ABSTRACT

Geoscientists infer past plate motions, which serve as fundamental constraints for a range of studies, from observations of magnetic isochrons as well as hotspots tracks on the ocean floor and, for stages older than the Cretaceous, from paleomagnetic data. These observations effectively represent time-integrals of past plate motions but, because they are made at present, yield plate kinematics naturally tied to a present-day reference-frame, which may be another plate or a hotspots system. These kinematics are therefore different than those occurred at the time when the rocks acquired their magnetisation or when hotspot-related marine volcanism took place, and are normally corrected for the reference-frame absolute motion (RFAM) that occurred since then. The impact of true-polar-wander events on paleomagnetic data and the challenge of inferring hotspot drifts result in RFAMs being less resolved – in a temporal sense – and prone to noise. This limitation is commonly perceived to hamper the correction of plate kinematic reconstructions for RFAMs, but the extent to which this may be the case has not been explored. Here we assess the impact of uncertain RFAMs on kinematic reconstructions using synthetic models of plate motions over 100 million years. We use randomly-drawn models for the kinematics of two plates separated by a spreading ridge to generate a synthetic magnetisation pattern of the ocean floor. The kinematics we infer from such a pattern are outputs that we correct for synthetic RFAMs using two equivalent methods (a classical one as well as another that we propose and test here) and then compare to the 'true' motions input. We assess the misfits between true and inferred kinematics by exploring a statistically-significant number of models where we systematically downgrade the temporal resolution of RFAM synthetic data and add noise to them. We show that even poorly-resolved, noisy RFAMs are sufficient to retrieve reliable plate kinematic reconstructions. For relative (i.e., one plate with respect to another) and absolute (i.e., relative to the deep mantle) plate motions, estimates upon RFAM correction differ from the true kinematics by less that 10% and 3%, respectively.

1. Introduction

Reconstructions of past plate motions, whether relative to one another or absolute (i.e., with respect to a fixed reference-frame – typically the deep mantle), are important constraints for tectonic studies (e.g., Torsvik et al., 2010), mantle circulation models (e.g., Schuberth et al., 2009; Davies et al., 2012; Colli et al., 2015), studies of dynamic topography and associated sea-level (e.g., Moucha et al., 2008), inferences on torques acting on lithospheric plates (e.g., Bird et al., 2008; Copley et al., 2010; Austermann and Iaffaldano, 2013; Iaffaldano and Bunge, 2015), among others. One infers past relative motions of plates from reconstructions of their relative positions through time, based on the present-day magnetisation pattern of the ocean floor (e.g., Gordon and Jurdy, 1986; Dyment, 1993; DeMets et al., 1994; Gaina et al., 2013; Seton et al., 2014) and a geomagnetic polarity time scale (e.g., Cande and Kent, 1995; Lourens et al., 1995). Because young, hot crust recorded the polarity of Earth's magnetic field when it was accreted to the lithosphere along mid-oceanic ridges, one can estimate from the present-day magnetisation pattern how two plates separated by a spreading ridge have moved relative to each another since a particular time in the past, and thus reconstruct their past relative positions. These inferences, referred to as finite rotations, express the relative rotation between two plates over a finite interval of time that is known from the geomagnetic polarity time scale (Cox and Hart, 1986). Finite rotations effectively represent time integrals of plate motions. Geoscientists reconstruct the past relative positions of any two plates – particularly those on opposite sides

* Corresponding author.
E-mail address: giia@ign.ku.dk (G. Iaffaldano).

http://dx.doi.org/10.1016/j.epsl.2016.11.003
0012-821X/

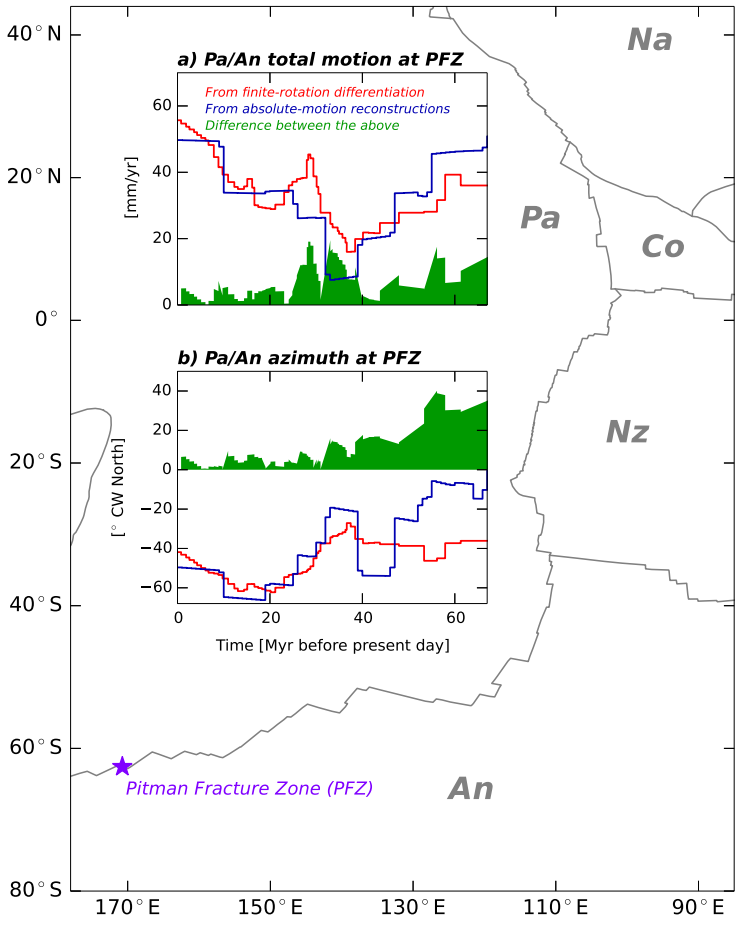

Fig. 1. Comparison of Pacific/Antarctica (Pa/An) relative motions along the Pitman Fracture Zone (PFZ) inferred from reconstructions of Pa and An absolute motions (blue) and from differentiation of Pa/An finite rotations (red). The upper inset shows the total motion, while the lower inset shows the azimuth of motion, in ° clockwise (CW) from North. The green areas show the absolute value of the difference between each kinematic parameter. Plate margins are in grey. Co, Na and Nz are Cocos, North America and Nazca plates, respectively. (For interpretation of the references to colour in this figure legend, the reader is referred to the web version of this article.)

of a convergent margin – by combining finite rotations of plate pairs along circuits that link one plate to the other. For instance, one may reconstruct the past position of India with respect to Eurasia from finite rotations along the India–Somalia–Antarctica–Nubia–North America–Eurasia circuit (e.g., Copley et al., 2010; van Hinsbergen et al., 2011). In addition, if the past position of one plate with respect to the deep mantle is inferred from hotspots tracks (e.g., Doubrovine and Tarduno, 2008; Tarduno et al., 2009) or paleomagnetic data (e.g., Torsvik and Cocks, 2004), these circuits allow inferring finite rotations for past absolute (i.e., relative to the deep mantle) positions, and thus past absolute motions (e.g., Torsvik et al., 2010).

From a single finite rotation, one may estimate an average of the instantaneous – that is, occurring over the shortest time interval one can possibly imagine – rotation axis, or pole, and angular velocity of motion. Such an estimate averages the actual instantaneous motion over an interval from the time associated with the finite rotation to the present. The rotation axis is assumed to be oriented along the axis about which the finite rotation occurred, while the angular velocity equals the rotated angle divided by the elapsed time. Similarly, from a series of temporally-consecutive finite rotations, one may derive intermediate finite rotations during consecutive stages – covering from the oldest reconstructed time to the present – and then infer the average instantaneous kinematics, also known as Euler vectors, during these consecutive stages (Cox and Hart, 1986), as described above. In the following, we will refer to such a method as finite-rotation differentiation. Geodynamicists are interested in stage Euler vectors of absolute (i.e., relative to the deep mantle) plate motions, because they enter the torque–balance equation of tectonic plates (Iaffaldano and Bunge, 2015), along with the torques controlling plate motions. Euler-vector variations through geological time are thus the prime constraint to study temporal changes in plate driving/resisting forces (e.g., Norabuena et al., 1999; Iaffaldano and Bunge, 2009; Copley et al., 2010). Similarly, stage Euler vectors of relative plate motions are important in order to study the past tectonic style of faults (e.g., Brune et al., 2016) or the structural evolution of Earth's crust (e.g., Wu et al., 2016), among others. However, the present-day magnetisation of the ocean floor and hotspots tracks allow direct inference of finite rotations, not stage Euler vectors. Geomagnetic reversals appear in the magnetisation pattern of the ocean floor as more-or-less defined lines, known as isochrons (literally, 'same age'). These formed as hot crust spreading out of ridges cooled below its Curie point and then travelled along with the associated plate, while the magnetic field reversed at times. Because geoscientists infer finite rotations from the present-day geography of isochrons (specifically, from observations of points along them called magnetic picks) and hotspots tracks, stage Euler vectors derived through finite-rotation differentiation are tied to a present-day reference frame. Therefore, they do not describe exactly the actual kinematics occurred when isochrons formed (Cox and Hart, 1986).

Fig. 1 illustrates such a discrepancy, or misfit, for the spreading motion between the Pacific and Antarctica plates. We chose this example because recent reconstructions (e.g., Croon et al., 2008; Wright et al., 2015), combined together, yield one of the longest

high-temporal-resolution records of relative finite rotations. Fig. 1a shows the total motion at the Pitman Fracture Zone, inferred by differentiating the noise-reduced (Iaffaldano et al., 2012, 2014a) finite rotations of Croon et al. (2008) and Wright et al. (2015) (red), and from reconstructions of the absolute motions of the Pacific and Antarctica plates (blue), using the GPlates tool (Gurnis et al., 2012) and the finite-rotations collection by Gibbons et al. (2015). Fig. 1b shows the associated azimuth of motion in the two cases. For simplicity, we use the absolute value of the difference between these kinematic parameters (shown in green) to indicate the misfit between actual kinematics (i.e., derived from the Pacific and Antarctica absolute motions) and those inferred through finite-rotation differentiation. Because the temporal resolution of the two records is different, some misfit is expected. However, had resolution been the only source of differences, the misfits would be more or less constant through geological time. This would apply also for kinematic reconstructions with respect to a hotspots reference frame. Instead, it is evident that the records differ increasingly at older stages – misfits increase backwards in time, indicating additional sources of discrepancy. Plate kinematicists are familiar with such misfits. For relative plate motions, they arise because isochrons observed at present and used as reference frames to infer finite rotations have moved, with respect to the deep mantle, since the time they formed, according to the absolute motion of the plate to which they belong. Similarly, for plate motions relative to hotspots reference frames, misfits arise because hotspots are not fixed, but rather drift with respect to the deep mantle (e.g., Davies and Davies, 2009), causing reference frames to move through time with respect to the tracks already left on Earth's surface. In Fig. 1, the Pitman Fracture Zone motion in blue features a correction for the reference-frame absolute motion (RFAM), while that in red does not.

It may seem intuitive to link the precision of RFAM corrections to the temporal resolution and accuracy of the reconstructed RFAMs, which are inferred from the age progression of hotspots tracks and paleomagnetic data from the Cretaceous and Jurassic. These typically feature a temporal resolution of 10–20 million years (Myr) (e.g., Gordon and Jurdy, 1986; Müller et al., 1993; Torsvik et al., 2010; Doubrovine et al., 2012). In contrast, recent reconstructions of relative finite rotations based on observations of the ocean-floor magnetisation patter resolve past relative positions and motions at a resolution of 1 Myr or less (e.g., Croon et al., 2008; Merkouriev and DeMets, 2006, 2008, 2014; Eagles and Wibisono, 2013). In addition to the non-fixity of hotspots, the possible impact of true polar wander on paleomagnetic records (e.g., Torsvik et al., 2012) make RFAM reconstructions challenging. Under such a premise, corrections for RFAMs may seem equally challenging. In this study we present a theoretical appraisal of the precision of these corrections when RFAMs are noisy and not as well resolved (in a temporal sense) as the records of plate motions relative to other plates or to hotspots systems. We use a statistically-significant number of synthetic calculations of spreading evolution in which we generate, and thus know, absolute (i.e., relative to the deep mantle) motions of two plates sharing a spreading ridge, from 100 Myr ago to the present. From these, we generate synthetic picks on the present-day isochrons that we use to infer finite rotations between the two plates and the resulting time series of stage Euler vectors for their relative motions – through finite-rotation differentiation. We then correct the relative kinematics using as RFAM a coarser, noisy version of the absolute motion of the plate to which the reference-frame for relative motion is anchored. Our synthetic calculations feature angular velocities comparable to those of the relative motions between plates, as well as those typical of the kinematics of a plate with respect to a slow plate or to a moving hotspots system. This lets us draw inferences relevant to both relative and absolute plate motions. These simulations take advantage of the fact that we can perform finite-rotation differentiation in a synthetic setting where true absolute and relative motions are known. Therefore, we appraise the impact of uncertain (i.e., noisy and relatively-poorly resolved) RFAMs on kinematic reconstructions by comparing the true kinematics with those obtained upon differentiation and RFAM correction, using two equivalent methods: the classical one that requires finite-rotation combination, differentiation and vector summation (Cox and Hart, 1986), as well as an alternative, equivalent procedure. Lastly, we address the implications for surface plate velocities.

2. Kinematics of two neighbouring plates sharing a spreading ridge

We consider a ridge – referred to as R – separating two imaginary plates A and B that starts spreading 100 Myr before present. We generate a series of 100 stage Euler vectors $\vec{\omega}_{Ak}$ for the absolute (i.e., relative to the deep mantle) motion of A. The index $k = 1, ..., 100$ identifies each 1-Myr-long stage, with $k = 1$ closest to the present. We change the kinematics of A every 5 Myr, in line with evidence from noise-reduced finite-rotation data sets (e.g. Iaffaldano et al., 2012, 2014b; DeMets et al., 2015). Thus, $\vec{\omega}_{Ak}$ has the same value for $k = 1, ..., 5$, a different value for $k = 6, ..., 10$, yet a different value for $k = 11, ..., 15$, and so on. For the absolute motion of plate A, the angular velocity during each 5-Myr-long stage is randomly selected in the range from 0.1 to 1°/Myr, consistent with reconstructed absolute plate motions since the Cretaceous (Torsvik et al., 2010). Doing so yields absolute plate velocities up to 11 cm/yr. The longitude and latitude of the Euler pole during each stage is randomly assigned within a $40° \times 40°$ region, whose centre is also randomly selected on Earth's surface, but remains fixed during the entire model time (100 Myr). For the absolute motion of plate B, we set the time series of stage Euler vectors $\vec{\omega}_{Bk}$ in the same way, but independently of $\vec{\omega}_{Ak}$. Because we use the synthetic magnetisation pattern on plate B as the reference frame for inferring relative finite rotations, we also introduce the possibility of setting its angular velocity in range from 0.1 to 0.2°/Myr. This lets us simulate a slower-than-usual RFAM (absolute velocities up to 2 cm/yr) that better mimics the velocities of relatively-slow plates like Africa and Eurasia, or the inferred drift-rates of hotspots (e.g., Richards and Griffiths, 1988; Davies and Davies, 2009), both of which are often used as reference frame in kinematic reconstructions. Furthermore, such a range of angular velocities is in line with previous findings on the motions of hotspots reference frames. For instance, O'Neill et al. (2005) inferred some 10° of motion of the Indo-Atlantic moving hotspots reference-frame with respect to the deep mantle for stages older than 80 Ma, which implies a RFAM of around 0.125°/Myr – on average – or more – if that motion was not accrued continuously through geological time. We assume that at any time R has the shape of the present-day Carlsberg Ridge, where India and Somalia diverge. This arbitrary choice has no impact on the kinematics of plates. We then use $\vec{\omega}_{Ak}$ and $\vec{\omega}_{Bk}$ to simulate the absolute motion of R by requiring that spreading be symmetric, so $\vec{\omega}_{Rk} = (\vec{\omega}_{Ak} - \vec{\omega}_{Bk})/2 + \vec{\omega}_{Bk}$. Because of this, the motion of A relative to R, $\vec{\omega}_{ARk} = \vec{\omega}_{Ak} - \vec{\omega}_{Rk}$, is always half that of A relative to B, $\vec{\omega}_{ABk} = \vec{\omega}_{Ak} - \vec{\omega}_{Bk}$. The shape of R is fixed, while its absolute (i.e., relative to the deep mantle) position – which we also track – changes through time consistently with $\vec{\omega}_{Rk}$. Incorporating spreading asymmetry and a ridge that changes shape would only add degrees of freedom to the problem, with no additional benefit to our goals. For simplicity, we assume that Earth's magnetic field reverses every 1 Myr and use $\vec{\omega}_{Ak}$, $\vec{\omega}_{Bk}$, $\vec{\omega}_{Rk}$ and the shape of R to generate synthetic isochrons. As model time goes by, we generate two isochrons – one on A, the other on B – every 1 Myr. From then, until the present, we use $\vec{\omega}_{Ak}$ and $\vec{\omega}_{Bk}$ to

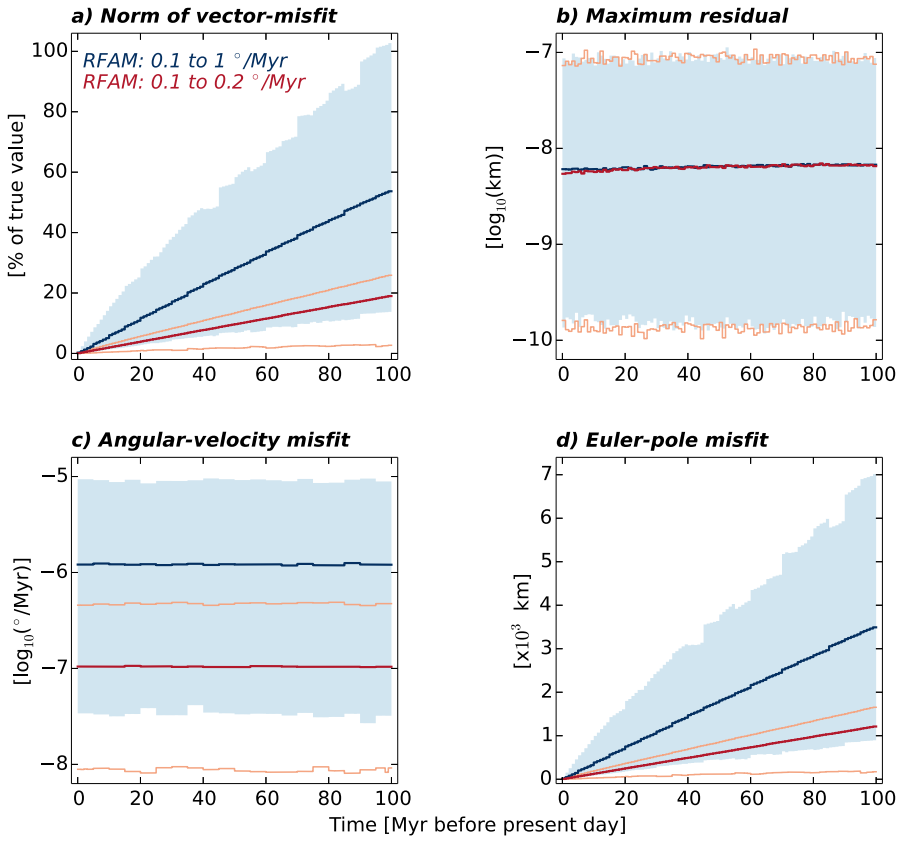

Fig. 2. Statistics for the comparison of true kinematics with those inferred from finite-rotation differentiation, prior to RFAM correction, for the ensemble of 5000 synthetic simulations of motion between plates A and B. In dark colour are ensemble averages, while light-colour areas/lines show the regions where 95% of the samples fall. Blue refers to the ensemble where RFAM is in range 0.1 to 1°/Myr, while red refers to the case where RFAM is in range 0.1 to 0.2°/Myr. a) Relative norm of the difference of stage Euler vectors – i.e., misfit – associated with true and inferred kinematics. b) Maximum geodesic distance – i.e., residual – between present-day synthetic picks of A and those rotated from their initial positions using the inferred finite rotations. c) Difference between angular velocities of true and inferred stage Euler vectors. d) Geodesic distance between Euler poles associated with true and inferred stage Euler vectors. (For interpretation of the references to colour in this figure legend, the reader is referred to the web version of this article.)

displace these isochrons on Earth's surface, but keep their shape fixed to fulfil the requirement of plate rigidity. We then sample the present position of each isochron at 50 points that mimic picks of the magnetic anomalies. After 100 Myr of model time, we use the 100 sets of two isochrons for every Myr to infer finite rotations for the past position of A relative to B. This involves an inversion for the matrix that rotates picks of A from their initial positions – that is, coinciding with those on B, to which the finite-rotation reference frame is therefore anchored – onto their present-day positions.

Various methods have been proposed to do this (e.g., Bullard et al., 1965; McKenzie and Sclater, 1971; Pilger, 1978; Hellinger, 1981), each featuring different benefits/drawbacks in relation to availability as well as quality of magnetic picks and their uncertainties. Here we use a procedure similar to that of Pilger (1978), which finds the rotation matrix that minimises the sum of squared misfits between picks. Since we deal with synthetic picks, we know exactly, for each pick on A, its conjugate on B. This knowledge eliminates the need for generating and mapping synthetic fracture zones of the ocean floor, and using the chord formed by the two closest picks in Pilger (1978)'s procedure. The supplementary information describes our inversion method, which yields both finite rotations and the maximum geodesic distance – or residual – between conjugate synthetic picks upon rotation. Next, we differentiate the set of 100 inferred finite rotations, which are – in Cox and Hart (1986)'s nomenclature – forward motion poles. These rotations, if used to generate a movie of their progression, would yield forward relative motions causing new ocean floor to spread out of the ridge. Therefore, their differentiation yields the time series of stage Euler vectors for the relative motion of A with respect to B, forward in time. We use the finite rotation associated with the most recent time to infer the Euler vector for the stage from that time to the present. This is equivalent to augmenting the set of finite-rotation matrices with the identity matrix for the rotation since 0 Myr ago. We refer to this series of Euler vectors as $\vec{\Omega}_{ABk}$, and compare them with the true stage Euler vectors for relative motion $\vec{\omega}_{ABk}$.

We repeat this test 5000 times, each time using new randomly-generated series of $\vec{\omega}_{Ak}$ and $\vec{\omega}_{Bk}$. Each test is a sample of an ensemble that we deem large enough for statistically meaningful inferences on plate-motion misfits. Fig. 2a shows the ensemble statistics for the relative norm of Euler–vector difference $|\vec{\omega}_{ABk} - \vec{\Omega}_{ABk}|/|\vec{\omega}_{ABk}|$, which quantifies as a single scalar value the discrepancy between reconstructed and true kinematics. Dark colours show ensemble averages, while light-colour areas/lines show the ranges where 95% of the samples fall and thus represent confidence intervals on the averages. We take these estimates as representative of the misfits associated with finite-rotation differentiation over a period of 100 Myr prior to the present, when no correction for RFAM is performed. Blue refers to the ensemble where the RFAM angular velocity is in range from 0.1 to 1°/Myr, while red refers to the ensemble where this is in range from 0.1 to 0.2°/Myr. These ranges imply that the former ensemble provides an indication of misfits associated with fast relative plate motions since the Late Mesozoic, while the latter better fits the case of plate motions relative to slow plates or to moving hotspots systems.

In fact, from a mathematical viewpoint, past positions of a plate relative to another plate or to a hotspots system are both expressed by finite rotations. This means that in our models there is no need to also generate synthetic hotspots tracks on the ocean floor in order to infer synthetic past absolute positions of plate B, to which the reference frame for relative motion is attached. Knowledge of the past positions of R – which we track in our models – serves this purpose. As one should expect, misfits become progressively larger for older stages. For fast (0.1 to 1°/Myr) RFAM, they can exceed 50% of the true relative motion back to times like the Early Cenozoic or Late Mesozoic. Fig. 2b demonstrates that misfits do not arise from the inversion method we use for inferring finite rotations from synthetic picks of each stage. We show the ensemble-average maximum residual between present-day positions of picks on plate A and the rotated initial positions of the same. Within the 95% confidence intervals – light-colour areas/lines – these residuals do not increase for older stages – as the misfits in panel a do – and are too small to explain the misfit magnitude. Instead, these small residuals are associated with the precision of the computer used for our calculations. Figs. 2c–d further analyse the misfits: panel c shows the average absolute value of the difference in angular velocities, $|\vec{\omega}_{ABk}| - |\vec{\Omega}_{ABk}|$, while panel d shows the geodesic distance between the Euler poles for $\vec{\omega}_{ABk}$ and $\vec{\Omega}_{ABk}$. The former is very small, about 6 orders of magnitude smaller than the true angular velocities. Therefore, misfits in panel a arise mainly from the fact that stage Euler poles are reconstructed in different positions than the true ones, as evidenced by statistics in Fig. 2d. Such a misplacement becomes progressively larger for older stages, indicating that misfits result largely from the present geographical positions of the conjugate isochrons – which impact the rotation poles – rather than the angular distance between them – which impacts the angular velocity.

3. Accounting for RFAM: data resolution and noise

These analyses are consistent with the fact that RFAM occurred while relative rotations between plate and reference frame accrued, thus generating a misfit between true kinematics and those obtained from finite-rotation differentiation. One may correct these misfits using either of two equivalent procedures, both of which require knowledge of the RFAM in the form of finite rotations for the past absolute (i.e., relative to the deep mantle) positions of the reference frame. In our synthetic simulations, we obtain them using knowledge of the past positions of R in addition to the synthetic magnetic picks. In reality, however, RFAM finite rotations require hotspots tracks or paleomagnetic data, and are therefore less resolved – in a temporal sense – and prone to noise. The first, classical procedure consists of combining the reference-frame absolute finite-rotations with those expressing past relative positions between plate and reference frame, in order to obtain past absolute plate positions, past absolute motions of plate and reference frame, and thus the correct relative motions between plate and reference frame. Such a procedure involves a few iterations of finite-rotation differentiation/addition – using matrix algebra – and vector summation (Cox and Hart, 1986). The second procedure, which we propose and test here, requires one differentiation and one combination of finite rotations: it consists of rotating the stage Euler poles of relative motion inferred through differentiation by an amount equal to the time-integral of the opposite of the RFAM, from the time associated with the stage in question to the present.

We use the ensembles described at the end of Section 2 to test the extent to which coarse temporal resolution of RFAM reconstructions impacts the inference of plate/reference-frame kinematics. To this end, we correct for RFAM by post-processing the stage Euler poles for relative motion that have been inferred through finite-rotation differentiation, $\vec{\Omega}_{ABk}$, following the latter of the two procedures. We indicate with $\vec{\gamma}_B$ the series of stage Euler vectors for the absolute motion of B, to which the reference frame is anchored. $\vec{\gamma}_B$ spans the same time period of $\vec{\omega}_{Bk}$, but differs from it in that it features a smaller number of vectors. This mimics a coarser temporal resolution of RFAMs compared to the relative kinematics inferred from the finite rotations set. We refer to the length of the temporal stages associated with $\vec{\gamma}_B$ as Δt_B, to the unit vectors associated with the absolute Euler poles as $\vec{p}_B$, and to the absolute angular velocities as γ_B. Similarly, $\vec{r}_{ABk}$ indicates the unit vectors of the Euler poles associated with $\vec{\omega}_{ABk}$. Lastly, we indicate with $\mathbf{R}(\vec{u}, \theta)$ the matrix describing a rigid rotation of an angle θ about the axis $\vec{u}$. We rotate the stage Euler poles $\vec{r}_{ABk}$ obtained through finite-rotation differentiation into $\vec{r}'_{ABk}$ as follows: assuming that the first m vectors of the series $\vec{\gamma}_B$ span the period from the present back to the k-th stage of $\vec{r}_{ABk}$, then

$$\vec{r}'_{ABk} = \mathbf{R}(\vec{p}_{Bm}, -\gamma_{Bm}\Delta t_{Bm})\mathbf{R}(\vec{p}_{B(m-1)}, -\gamma_{B(m-1)}\Delta t_{B(m-1)})\ldots \mathbf{R}(\vec{p}_{B1}, -\gamma_{B1}\Delta t_{B1})\vec{r}_{ABk} \quad (1)$$

Since the absolute motion of B is in fact known from its finite rotations with respect to the deep mantle, we note that the sum (as defined by the algebra of rotation matrices) of stage rotations in the formula above is always equal to the sum of one of the finite rotations and a fraction of its temporally-preceding one. This would be the case also for real reconstructions. We refer to the stage Euler vectors of relative motions upon post-processing as $\vec{\Omega}'_{ABk}$. They feature the same angular velocities of $\vec{\Omega}_{ABk}$, but stage poles modified according to Eq. (1). To apply the post-processing described above to the ensembles of Section 2, in each sample we first obtain a coarser-temporal-resolution selection of finite rotations for the past absolute position of B by taking one every T Myr from the 100 synthetically-generated rotations. Next, we differentiate this series and use the obtained stage Euler vectors as $\vec{\gamma}_{Bn}$ in Eq. (1). Figs. 3a–c show the relative norm of the Euler-vector misfit $|\vec{\omega}_{ABk} - \vec{\Omega}'_{ABk}|/|\vec{\omega}_{ABk}|$ for values of T equal to 10, 20 and 50 Myr in our ensembles. We show results for the cases where RFAM angular velocities are in ranges from 0.1 to 1°/Myr (blue) and from 0.1 to 0.2°/Myr (red). In the supplementary information we show the same statistics, obtained using the classical method for RFAM correction. They are the same as those in Fig. 3, and hence demonstrate the equivalence of the two methods. The misfits are now significantly smaller than those inferred prior to post-processing. The inferred kinematics better match the true ones for smaller values of T, which is justified by noting that averaging the RFAM over shorter periods better captures the actual motion, and thus provides a more precise correction for the locations of stage Euler poles at any point in the geological past. This is also reflected in the periodicity that the improved misfits exhibit. Nonetheless, even when we set $T = 50$ Myr (Fig. 3c) and use just two Euler vectors for the series $\vec{\gamma}_B$ to mimic a much coarser temporal resolution than any absolute-motion reconstruction available (e.g., Gordon and Jurdy, 1986; Torsvik et al., 2010), the stage Euler vectors after post-processing match the true kinematics significantly better than the originally-inferred ones. Regardless of the value we assign to T, the worst-case scenario is one where average misfits never exceed 3% and may thus be deemed negligible compared to other sources of uncertainty.

Next, we assess the extent to which noise in RFAM impacts the correction and thus the inference of true kinematics. We repeat the tests performed to explore the effect of coarser temporal resolution of RFAM, but introduce random noise in RFAM data. To this end, we perturb the longitude, latitude and angle of the finite rotations for the past absolute positions of B by random values. Longitude and latitude of the finite-rotation subsets are perturbed by up to 5°, while the rotated angle is perturbed by up to 0.5°.

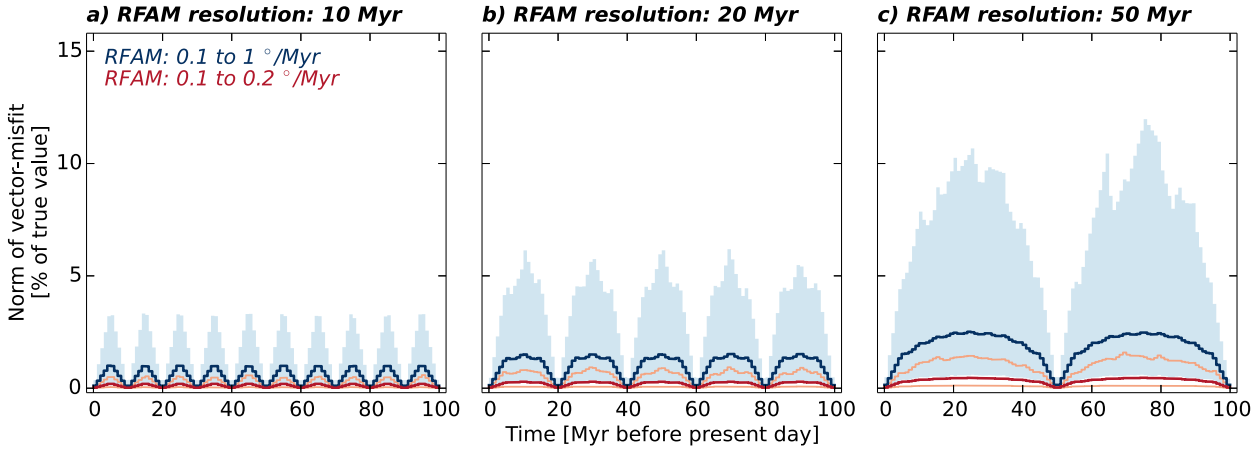

Fig. 3. Same as Fig. 2a, but for correction of the inferred stage Euler vectors for RFAM, when the latter is resolved every 10 (a), 20 (b) and 50 (c) Myr. (For interpretation of the colours in this figure, the reader is referred to the web version of this article.)

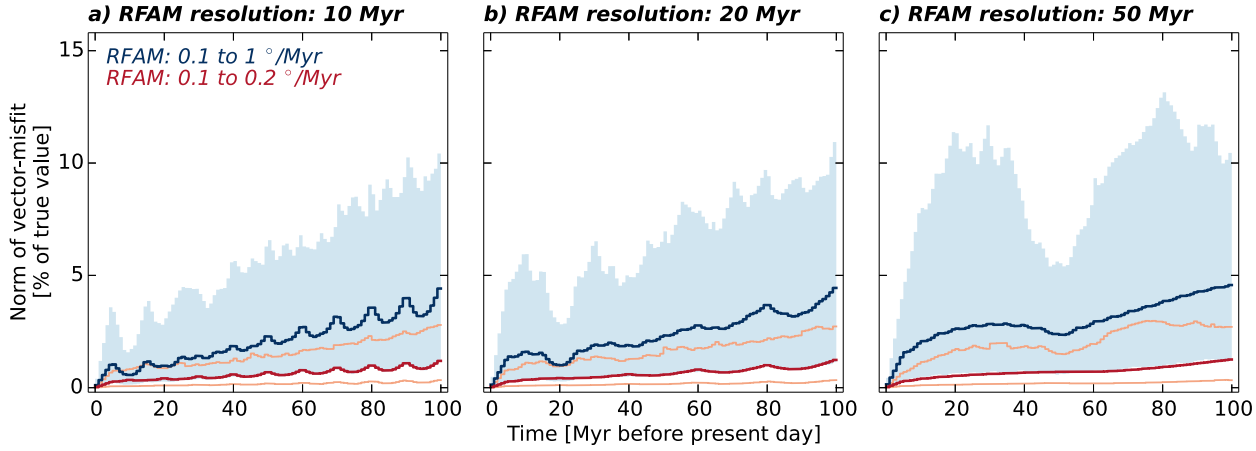

Fig. 4. Same as Fig. 3, but for correction of the inferred stage Euler vectors using a noisy version of the RFAMs. (For interpretation of the colours in this figure, the reader is referred to the web version of this article.)

These perturbation values are in line with results from studies of noise reduction through transdimensional hierarchical Bayesian Inference (e.g., Malinverno, 2002; Sambridge et al., 2006; Bodin and Sambridge, 2009) in real finite rotations for past plate positions since the Mid-Cenozoic (e.g. Iaffaldano et al., 2012, 2014b; DeMets et al., 2015). Results from these tests, shown in Fig. 4a–c (see the supplementary information for the results obtained using the classical method for RFAM correction), indicate that even by using a noisy RFAM record, one may still arrive at an acceptable estimate of the true kinematics: when RFAM angular velocities are in the range from 0.1 to 1°/Myr (blue in Fig. 4), average misfits never exceed 5% of the true kinematics, although some of the samples feature misfits around 10%. When RFAM angular velocities are in range from 0.1 to 0.2°/Myr (red), misfits never exceed 3%, indicating that even coarse, noisy knowledge of RFAMs is sufficient for reliable estimates of absolute plate kinematics. Unlike in Fig. 3, the misfits in Fig. 4 remain similar despite RFAMs being less resolved as one moves from panel a to c. This owes to the trade-off between the impacts of RFAM resolution and noise. Finite-rotation noise is known to hamper the inferred plate kinematics progressively more as the temporal resolution improves (e.g., Iaffaldano et al., 2013). For example, the same amount of noise added to a finite rotation for the past 2 Myr will have a larger impact on the inferred kinematics than if the same rotation instead occurred over 10 Myr. On the contrary, RFAM corrections improve for better-resolved RFAMs, as evident from Fig. 3. Therefore, when the two effects are combined, misfits tend to remain similar.

Because the surface motions associated with angular velocities in range from 0.1 to 0.2°/Myr are similar to the inferred drift-rates of hotspots, the statistics in red in Fig. 4 are particularly relevant to reconstructions of absolute (i.e., relative to the deep mantle) plate motions, on which studies concerning dynamic topography (e.g., Braun, 2010; Flament et al., 2013), the adjoint method in mantle convection (e.g., Ghelichkhan and Bunge, 2016) or mantle heterogeneity structures (e.g., Shephard et al., 2012) rely. This motivated us to explore the magnitude of the misfits between true and inferred surface velocities associated with these stage Euler vectors. We start by randomly generating, for each samples used in exploring the impact of noise, a position $\vec{x}$ on Earth's surface 50° to 140° away from the average Euler pole over the 100 Myr of model time. This is in line with the observation that rigid plates typically feature Euler poles located around 90° away from their center of mass (Gordon, 1998), and implies surface velocities in range from 10 to 130 mm/yr. We then calculate the time series of inferred surface velocities $\vec{v}'_{ABk} = \vec{\Omega}'_{ABk} \times \vec{x}$ and compare it to the series of true velocities $\vec{v}_{ABk} = \vec{\omega}_{ABk} \times \vec{x}$. Fig. 5a shows the difference in total motion – that is, the absolute value of $(|\vec{v}'_{ABk}| - |\vec{v}_{ABk}|)$ – for cases where corrections to the kinematics inferred through differentiation are performed using RFAM resolved at 10 (brown) and 20 (green) Myr. Fig. 5b shows the angular separation between the directions of inferred and true motions. Misfits of total motions are lower than 2 mm/yr, which means they are negligible compared to other sources of uncertainty. However, misfits of velocity directions, while negligible on average, in some cases exceed 20°.

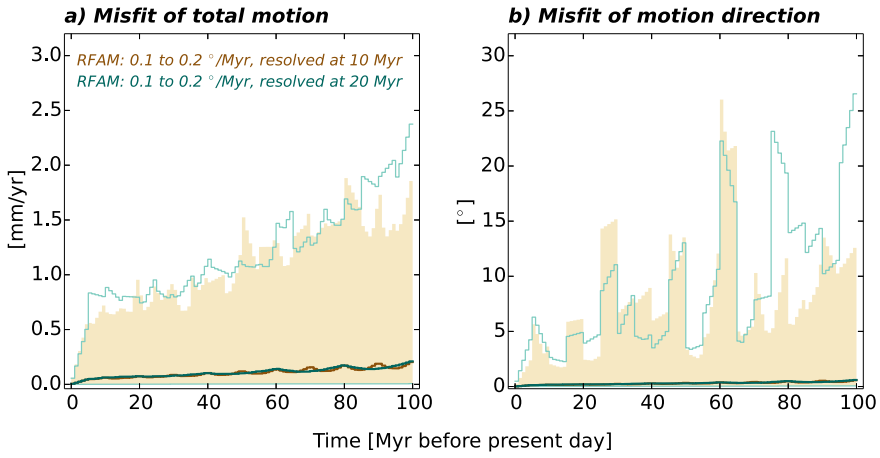

Fig. 5. Statistics for the comparison of true surface motions with those inferred by finite-rotation differentiation and correction for RFAM, when the latter is in range from 0.1 to 0.2°/Myr and resolved at 10 (brown) and 20 (green) Myr. Ensemble averages are in dark colour, while light-colour areas/lines show the 95% confidence regions. a) Misfit of total motions. b) Angular distance between motion directions. (For interpretation of the references to colour in this figure legend, the reader is referred to the web version of this article.)

This may have implications, for instance, for studies of the past style (convergent, divergent or transform) of tectonic margins (e.g., Boschman and van Hinsbergen, 2016) or when comparing deep-mantle structures inferred from seismic tomography with those predicted in mantle circulation models, which use reconstructions of absolute plate motions over the past 100 to 200 Myr as top-boundary kinematic conditions (e.g., Domeier et al., 2016).

4. Conclusions

We developed synthetic models of the temporal evolution of two plates separated by a spreading ridge over 100 Myr. In these models, absolute (i.e., relative to the deep mantle) plate motions were set as inputs and used to generate a synthetic pattern of ocean-floor magnetisation, and to track the past positions of a ridge. From these, we determined finite rotations for the past relative positions of plates, as well as for the absolute position of the reference frame. We differentiated relative finite-rotations to infer stage Euler vectors for the relative motions, and compared them to the true kinematics. Failing to account for reference-frame absolute motions (RFAMs) in range from 0.1 to 0.2°/Myr, which is comparable to the velocities of slow-moving plates or to hotspots drift-rates, can lead to relative misfits between inferred and true kinematics of around 20%. However, when RFAMs are in range from 0.1 to 1°/Myr, which is typical of fast tectonic plates, relative misfits can reach 50% or more. Corrections for RFAM can be performed following two equivalent procedures. We assessed how the coarse temporal resolution that is typical of RFAM records (compared to relative plate-motion records) impacts the correction of plate/reference-frame motions. Furthermore, we explored the additional impact of RFAM data noise on these corrections. We found that even coarse, noisy RFAMs are nonetheless adequate to retrieve accurate estimates of the relative (i.e., one plate with respect to another) kinematics that depart from the true ones by less than 10%. For absolute (i.e., relative to the deep mantle) plate kinematics, misfits decrease to less than 3%.

Acknowledgements

We are very grateful to the Editor, Peter Shearer, and two anonymous reviewers for their constructive comments.

Appendix A. Supplementary material

Supplementary material related to this article can be found online at http://dx.doi.org/10.1016/j.epsl.2016.11.003.

References

Austermann, J., Iaffaldano, G., 2013. The role of the Zagros orogeny in slowing down Arabia–Eurasia convergence since ∼5 ma. Tectonics 32, 351–363.
Bird, P., Liu, Z., Rucker, W.K., 2008. Stresses that drive the plates from below: definitions, computational path, model optimization, and error analysis. J. Geophys. Res. 113, B11406.
Bodin, T., Sambridge, M., 2009. Seismic tomography with the reversible jump algorithm. Geophys. J. Int. 178, 1411–1436.
Boschman, L.M., van Hinsbergen, D.J.J., 2016. On the enigmatic birth of the Pacific Plate within the Panthalassa Ocean. Sci. Adv. 2, e1600022.
Braun, J., 2010. The many surface expressions of mantle dynamics. Nat. Geosci. 3, 825–833.
Brune, S., Williams, S.E., Butterworth, N.P., Müller, R.D., 2016. Abrupt plate accelerations shape rifted continental margins. Nature 536, 201–204.
Bullard, E., Everett, J., Smith, A., 1965. The fit of the continents around the Atlantic. Philos. Trans. R. Soc. Lond. A 258 (1088), 41–51.
Cande, S.C., Kent, D.V., 1995. Revised calibration of the geomagnetic polarity timescale for Late Cretaceous and Cenozoic. J. Geophys. Res. 100, 6093–6095.
Colli, L., Bunge, H.-P., Schuberth, B.S.A., 2015. On retrodictions of global mantle flow with assimilated surface velocities. Geophys. Res. Lett. 42.
Copley, A., Avouac, J.-P., Royer, J.-Y., 2010. India–Asia collision and the Cenozoic slowdown of the Indian plate: implications for the forces driving plate motions. J. Geophys. Res. 115, B03410.
Cox, A., Hart, R.B., 1986. Plate Tectonics: How It Works. Blackwell Scientific Publications.
Croon, M.B., Cande, S.C., Stock, J.M., 2008. Revised Pacific-Antarctic plate motions and geophysics of the Menard Fracture Zone. Geochem. Geophys. Geosyst. 9, Q07001.
Davies, D.R., Davies, J.H., 2009. Thermally-driven mantle plumes reconcile multiple hot-spot observations. Earth Planet. Sci. Lett. 278, 50–54.
Davies, D.R., Goes, S., Davies, J.H., Schuberth, B.S.A., Bunge, H.-P., Ritsema, J., 2012. Reconciling dynamic and seismic models of Earth's lower mantle: the dominant role of thermal heterogeneity. Earth Planet. Sci. Lett. 353–354, 253–269.
DeMets, C., Gordon, R.G., Argus, D., Stein, S., 1994. Effects of recent revisions of the geomagnetic reversal time scale on estimates of current plate motions. Geophys. Res. Lett. 21, 2191–2194.
DeMets, C., Merkouriev, S., Sauter, D., 2015. High-resolution estimates of Southwest Indian Ridge plate motions, 20 Ma to present. Geophys. J. Int. 203, 1495–1527.
Domeier, M., Doubrovine, P.V., Torsvik, T.H., Spakman, W., Bull, A.L., 2016. Global correlation of lower mantle structure and past subduction. Geophys. Res. Lett. 43, 4945–4953.
Doubrovine, P.V., Steinberger, B., Torsvik, T.H., 2012. Absolute plate motions in a reference frame defined by moving hot spots in the Pacific, Atlantic, and Indian oceans. J. Geophys. Res. 117, B09101.
Doubrovine, P.V., Tarduno, J., 2008. A revised kinematic model for the relative motion between Pacific oceanic plates and North America since the Late Cretaceous. J. Geophys. Res. 113, B12101.
Dyment, J., 1993. Evolution of the Indian triple junction between 65 and 49 Ma (Anomalies 28 to 21). J. Geophys. Res. 98, 13863–13877.
Eagles, G., Wibisono, A.D., 2013. Ridge push, mantle plumes and the speed of the Indian plate. Geophys. J. Int. 194, 670–677.
Flament, N., Gurnis, M., Müller, R.D., 2013. A review of observations and models of dynamic topography. Lithosphere 5, 189–210.

Gaina, C., Torsvik, T.H., van Hinsbergen, D.J.J., Medvedev, S., Werner, S.C., Labails, C., 2013. The African plate: a history of oceanic crust accretion and subduction since the Jurassic. Tectonophysics 604, 4–25.
Ghelichkhan, S., Bunge, H.-P., 2016. The compressible adjoint equations in geodynamics: derivation and numerical assessment. GEM Int. J. Geomath. 7, 1–30.
Gibbons, A., Zahirovic, S., Müller, R.D., Whittaker, J., Yatheesh, V., 2015. A tectonic model reconciling evidence for the collisions between India, Eurasia and intra-oceanic arcs of the central–eastern Tethys. Gondwana Res. 28, 451–492.
Gordon, R.G., 1998. The plate tectonic approximation: plate nonrigidity, diffuse plate boundaries, and global plate reconstructions. Annu. Rev. Earth Planet. Sci. 26, 615–642.
Gordon, R.G., Jurdy, D.M., 1986. Cenozoic global plate motions. J. Geophys. Res. 91, 12389–12406.
Gurnis, M., Turner, M., Zahirovic, S., DiCaprio, L., Spasojevic, S., Muller, R.D., Boyden, J., Seton, M., Maneaa, V.C., Bower, D.J., 2012. Plate tectonic reconstructions with continuously closing plates. Comput. Geosci. 38, 35–42.
Hellinger, S.J., 1981. The uncertainties of finite rotations in plate tectonics. J. Geophys. Res. 86, 9312–9318.
Iaffaldano, G., Bodin, T., Sambridge, M., 2012. Reconstructing plate-motion changes in the presence of finite-rotations noise. Nat. Commun. 3, 1048.
Iaffaldano, G., Bodin, T., Sambridge, M., 2013. Slow-downs and speed-ups of India–Eurasia convergence since ∼20 ma: data-noise, uncertainties and dynamic implications. Earth Planet. Sci. Lett. 367, 146–156.
Iaffaldano, G., Bunge, H.-P., 2009. Relating rapid plate-motion variations to plate-boundary forces in global coupled models of the mantle/lithosphere system: effects of topography and friction. Tectonophysics 474, 393–404.
Iaffaldano, G., Bunge, H.-P., 2015. Rapid plate motion variations: observations serving geodynamic interpretation. Annu. Rev. Earth Planet. Sci. 43, 571–592.
Iaffaldano, G., Hawkins, R., Bodin, T., Sambridge, M., 2014a. REDBACK: open-source software for efficient noise-reduction in plate kinematic reconstructions. Geochem. Geophys. Geosyst. 15, 1663–1670.
Iaffaldano, G., Hawkins, R., Sambridge, M., 2014b. Bayesian noise-reduction in Arabia/Somalia and Nubia/Arabia finite rotations since ∼20 ma: implications for Nubia/Somalia relative motion. Geochem. Geophys. Geosyst. 15, 845–854.
Lourens, L., Hilgen, F.J., Laskar, J., Shackleton, N.J., Wilson, D., 1995. In: A Geologic Time Scale. Cambridge University Press, London, pp. 409–440.
Malinverno, A., 2002. Parsimonious Bayesian Markov chain Monte Carlo inversion in a nonlinear geophysical problem. Geophys. J. Int. 151, 675–688.
McKenzie, D.P., Sclater, J.G., 1971. The evolution of the Indian Ocean since the late Cretaceous. Geophys. J. R. Astron. Soc. 24, 437–528.
Merkouriev, S., DeMets, C., 2006. Constraints on Indian plate motion since 20 ma from dense Russian magnetic data: implications for Indian plate dynamics. Geochem. Geophys. Geosyst. 7 (2), Q02002.
Merkouriev, S., DeMets, C., 2008. A high-resolution model for Eurasia–North America plate kinematics since 20 ma. Geophys. J. Int. 173, 1064–1083.
Merkouriev, S., DeMets, C., 2014. High-resolution Quaternary and Neogene reconstructions of Eurasia–North America plate motion. Geophys. J. Int. 198, 366–384.
Moucha, R., Forte, A.M., Mitrovica, J.X., Rowley, D.B., Quere, S., Simmons, N.A., Grand, S.P., 2008. Dynamic topography and long-term sea-level variations: there is no such thing as a stable continental platform. Earth Planet. Sci. Lett. 271, 101–108.
Müller, R.D., Royer, J.-Y., Lawver, L.A., 1993. Revised plate motions relative to the hotspots from combined Atlantic and Indian Ocean hotspot tracks. Geology 21, 275–278.
Norabuena, E.O., Dixon, T.H., Stein, S., Harrison, C.G.A., 1999. Decelerating Nazca-South America and Nazca-Pacific plate motions. Geophys. Res. Lett. 26, 3405–3408.
O'Neill, C., Müller, R., Steinberger, B., 2005. On the uncertainties in hot spot reconstructions and the significance of moving hot spot reference frames. Geochem. Geophys. Geosyst. 6, Q04003.
Pilger, R., 1978. A method for finite plate reconstructions with applications to Pacific-Nazca plate evolution. Geophys. Res. Lett. 5, 469–472.
Richards, M.A., Griffiths, R.W., 1988. Deflection of plumes by mantle shear flow: experimental results and simple theory. Geophys. J. 94, 367–376.
Sambridge, M., Gallagher, K., Jackson, A., Rickwood, P., 2006. Trans-dimensional inverse problems, model comparison and the evidence. Geophys. J. Int. 167, 528–542.
Schuberth, B.S.A., Bunge, H.-P., Steinle-Neumann, G., Moder, C., Oeser, J., 2009. Thermal versus elastic heterogeneity in high-resolution mantle circulation models with pyrolite composition: high plume excess temperatures in the lowermost mantle. Geochem. Geophys. Geosyst. 10, Q01W01.
Seton, M., Whittaker, J., Wessel, P., Mueller, R.D., DeMets, C., Merkouriev, S., Cande, S., Gaina, C., Eagles, G., Granot, R., Stock, J., Wright, N., Williams, S., 2014. Community infrastructure and repository for marine magnetic identifications. Geochem. Geophys. Geosyst. 15, 1629–1641.
Shephard, G.E., Bunge, H.-P., Schuberth, B.S.A., Müller, R.D., Talsma, A.S., Moder, C., Landgrebe, T.C.W., 2012. Testing absolute plate reference frames and the implications for the generation of geodynamic mantle heterogeneity structure. Earth Planet. Sci. Lett. 317–318, 204–217.
Tarduno, J., Bunge, H.-P., Sleep, N., Hansen, U., 2009. The bent Hawaiian–Emperor hotspot track: inheriting the mantle wind. Science 324, 50–53.
Torsvik, T.H., Cocks, L.R.M., 2004. Earth geography from 400 to 250 Ma: a palaeomagnetic, faunal and facies review. J. Geol. Soc. Lond. 161, 555–572.
Torsvik, T.H., der Voo, R.V., Preeden, U., Niocaill, C.M., Steinberger, B., Doubrovine, P.V., van Hinsbergen, D.J.J., Domeier, M., Gaina, C., Tohver, E., 2012. Phanerozoic polar wander, palaeogeography and dynamics. Earth-Sci. Rev. 114, 325–368.
Torsvik, T.H., Steinberger, B., Gurnis, M., Gaina, C., 2010. Plate tectonics and net lithosphere rotation over the past 150 my. Earth Planet. Sci. Lett. 291, 106–112.
van Hinsbergen, D.J.J., Steinberger, B., Doubrovine, P.V., Gassmöller, R., 2011. Acceleration and deceleration of India–Asia convergence since the Cretaceous: roles of mantle plumes and continental collision. J. Geophys. Res. 116, B06101.
Wright, N.M., Müller, R.D., Seton, M., Williams, S.E., 2015. Revision of Paleogene plate motions in the Pacific and implications for the Hawaiian–Emperor bend. Geology 43, 455–458.
Wu, J., Suppe, J., Lu, R., Kanda, R., 2016. Philippine Sea and East Asian plate tectonics since 52 Ma constrained by new subducted slab reconstruction methods. J. Geophys. Res. 121, 4670–4741.